Cryogenic considerations for superconducting magnet design for the material plasma exposure experiment

R C Duckworth[1], J A Demko[2], A Lumsdaine[1], J Rapp[1], T Bjorholm[1], R H Goulding[1], J B O Caughman[1], & W D McGinnis[1]

[1]Fusion and Materials for Nuclear Systems Division
Oak Ridge National Laboratory, Oak Ridge, TN 37831 USA

[2]Department of Mechanical Engineering
LeTourneau University, Longview, TX 75607

E-mail: duckworthrc@ornl.gov

Abstract. In order to determine long term performance of plasma facing components such as diverters and first walls for fusion devices, next generation plasma generators are needed. A Material Plasma Exposure eXperiment (MPEX) has been proposed to address this need through the generation of plasmas in front of the target with electron temperatures of 1-15 eV and electron densities of 10^{20} to 10^{21} m^{-3}. Heat fluxes on target diverters could reach 20 MW/m^2. To generate this plasma, a unique radio frequency helicon source and heating of electrons and ions through Electron Bernstein Wave (EBW) and Ion Cyclotron Resonance Heating (ICRH) has been proposed. MPEX requires a series of magnets with non-uniform central fields up to 2 T over a 5-m length in the heating and transport region and 1 T uniform central field over a 1-m length on a diameter of 1.3 m. Given the field requirements, superconducting magnets are under consideration for MPEX. In order to determine the best construction method for the magnets, the cryogenic refrigeration has been analyzed with respect to cooldown and operational performance criteria for open-cycle and closed-cycle systems, capital and operating costs of these system, and maturity of supporting technology such as cryocoolers. These systems will be compared within the context of commercially available magnet constructions to determine the most economical method for MPEX operation. The current state of the MPEX magnet design including details on possible superconducting magnet configurations is presented.

1. Introduction

For future fusion power systems the ability to operate reliably and efficiently for long periods of time will ultimately determine the feasibility of fusion as a renewable, nuclear power source. One component of current tokamak-based designs for fusion power that impact the overall performance lifetime are plasma facing components (PFCs). These PFCs are expected to handle heat fluxes up to 10 MW/m^2 at steady state and 1 GW/m^2 transiently for 1 ms for edge localized modes or ELMs that are produced from instabilities in magnetic confinement of the plasma [1]. Progress has been made in several areas [2-5], however, important plasma material interaction (PMI) issues remain such as melt-

layer dynamics of metal PFCs, thermo-mechanical stress of PFCs from cyclic heat loads and ELM transients, and impact of neutron irradiation on PFC's long-term performance [6].

While one approach to answer PMI issues in PFCs is through the inclusion of PFCs into existing fusion devices such as the Joint European Torus (JET) in the United Kingdom, the Korea Superconducting Tokamak Advanced Reactor in South Korea, and DIII-D National Fusion Facility in the United States, a dedicated facility is needed to systematically study the PMI dynamics in PFCs in order to understand existing materials and allow for the development of new materials. The Material-Plasma Exposure eXperiment (MPEX) [6] at Oak Ridge National Laboratory (ORNL) is a linear-based, RF plasma generation approach that is designed to provide the environment to answer key PMI and PFC technical challenges. This paper provides an outline of the essential components of the current MPEX design with an emphasis on the superconducting magnet and cryogenic design that is currently under consideration to achieve a steady state density of $n_e \sim 10^{21}$ m^{-3} and T_e=1-15 eV.

2. Functional Aspects of MPEX

A conceptual layout for MPEX is given in figure 1. In addition to the five distinct regions, Helicon Source, Electron Cyclotron Heating (ECH), Ion Cyclotron Heating (ICH), RF Test Area, and Target Area, the vacuum systems that are needed to regulate the specific gas pressures at different points along MPEX are also shown in figure 1. The transport section that is downstream of the RF Test area is optional and will not be covered in the paper. While detailed descriptions of the different MPEX RF elements have been given elsewhere [7], a brief summary of each is given in context of the magnetic field requirements.

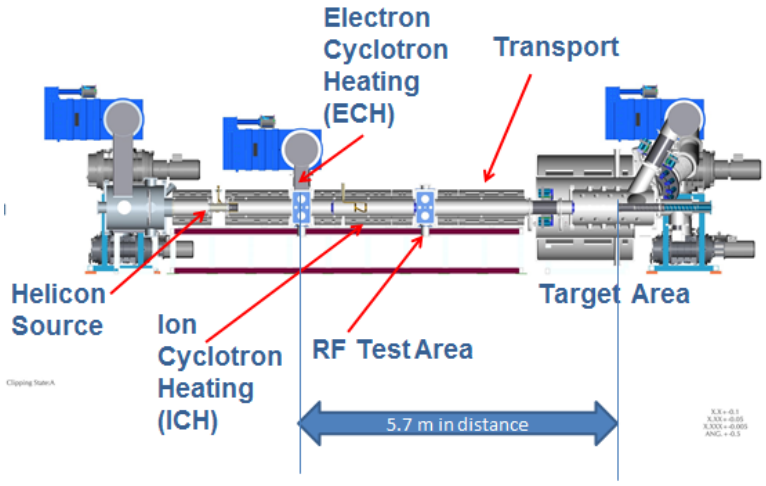

Figure 1. Conceptual drawing of MPEX

MPEX starts with a plasma source that utilizes a helicon antenna to couple electromagnetic waves through a 15-cm diameter aluminum nitride window to either hydrogen or deuterium at a frequency of 13.56 MHz [8-9]. With respect to magnet field, a uniform axial magnetic field of 0.6 T along the length of the window is required to prevent secondary harmonics from decreasing the plasma generation efficiency. After the helicon source, ECH occurs through a 200 kW, 28 GHz gyrotron Electron Bernstein waves into plasma that it is confined in a magnetic mirror with a minimum field of 1.6 T at the edges of the mirror and a minimum 0.6 T in the center.

Next, ICH uses single pass damping of slow electromagnetic waves from a modified Nagoya Type III antenna to launch rf waves over a high field region where the field is 1.8 T over 60 cm before the plasma transitions to lower field (1.6 T), 20 cm long region. This approach, which is often referred to as beach heating has been recognized as an efficient means to couple power into a single species plasma [10-14]. After the plasma passes through an RF Test Area, which amounts dimensionally and

functionally to a duplicate of ECH for the purposes of this study, it reaches the target area. The target area requires a uniform field, 1 T, over the entire target area, which is approximately 1-m long. This requirement is needed to assure that the plasma that is generated by the helicon and heated by the ICH and ECH can produce PMI conditions at target that are relevant to fusion environments. The current target cask design is approximately 1.5 m long with a diameter of 0.5 m. Given the instrumentation ports and the space that is needed for the diagnostic hardware such as feedthroughs and mirrors, the inner warm bore diameter of the target magnets was set to 1.15 m. In total, the entire length of the MPEX magnets is 10 m.

3. Superconducting Magnet Design Specifications

In order to accommodate the testing cycles on the order of hours to days for the effective study of PMI, a superconducting magnet design was selected. While there have been improvement in superconducting coils that have been fabricated from conductors such as magnesium diboride [15-16] and high temperature superconducting coated conductors [17-18], low temperature superconducting (LTS) wire, specifically NbTi, was selected for the magnet conductor. Specifically, the NbTi conductor was 0.75 mm diameter, copper matrix monolith with 54 filaments and a 1.3:1 copper to superconductor ratio from Oxford Instruments [19]. The conductor selection was driven by a preliminary risk assessment of the conductor performance as a function of field and temperature against the cost and maturity of the conductor manufacturing and supporting technologies like refrigeration.

The design of the MPEX magnets started with the physical dimensional constraints for each MPEX subsystem. The inner warm bore diameter for all the magnets except for the target magnets was set to 43.2 cm due to the 35.5-cm diameter vacuum piping and supporting cooling and hardware that runs along the axis of magnets between the helicon and target in figure 1. As stated earlier, the warm bore diameter of the target magnets was set to 115 cm. Assuming that the distance between the inner warm bore diameter and the inner diameter of the magnet is 8.1 cm to account for the supporting cryogenic structure, multilayer insulation, and mechanical supports, the inner magnet diameter of all magnets except the target magnet is 59.35 cm and the inner magnet diameter for the target magnets is 131 cm.

With respect to the axial separation of the magnets, it was assumed that between each sub-system, for example between the helicon and ECH & ICH and RF test area is 55.88 cm. It is assumed that 30.48 cm of this length is for hands-on access of room temperature connections between each sub-system with the remaining distance for vacuum insulation, cryostats, and axial mechanical supports. For the axial distances between magnets for subsystem based on their operating requirements, it was assumed that the axial distance between magnets was 66 cm for the ECH and RF test area and 71 cm for the helicon source. Figure 2 shows a scale schematic of the different separations with respect to the magnet assemblies for MPEX.

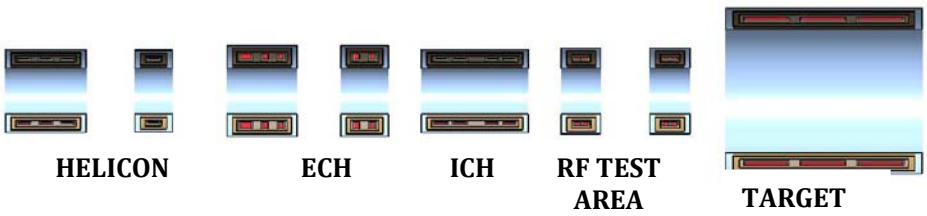

Figure 2. Scaled cross section view of MPEX magnets with different regions of MPEX operation highlighted. The diameter of the inner warm bore of the target magnet is 115 cm

With these physical constraints, initial coil widths, thicknesses, and engineering current densities were chosen for each coil to meet the field requirements for each sub-system. The target field profile along the axis for the MPEX magnets, which was modelled using a finite element software, FlexPDE

2D [18], is given in Figure 2. The field was then calculated in each coil and assuming an insulation percentage of 30% and each coil is cooled with liquid helium to a temperature of 4.2 K, the critical current in the coil was calculated and compared for the effective current for the coil. The properties of commercially available NbTi conductor [19] were used in conjunction with scaling factors in [21]. If the critical current of the coil exceeded 50% or an operating current was greater than 200 A was exceeded, the coil dimensions and current density were adjusted and the process repeated. The selection of an operating current of 200 A was based on commercially available, low voltage high current power supplies and minimizing the heat leak from the current leads of the cryogenic system. The goal for the configuration was to keep the current in each coil less than 200 A, minimize the number of turns, and assure that the forces of the magnets were within engineering limits of existing available structural materials. The peak hoop stress and axial forces between coils were calculated empirically with Wilson [22] guided by the mutual inductances as specified in Grover [23] to first order and were found to be in reasonable agreement to those values found numerically by FlexPDE. The peak hoop stress was between 0.40 MPa and 1.29 MPa and the axial forces were between 1.59 x 10^4 N and 1.63 x 10^6 N. The fraction of operating current to the coil critical current was between 0.15 and 0.50. Table 1 summarizes the key parameters for the twenty separate LTS magnets that are proposed for use in MPEX. It should be noted that the coil parameters described in Table 1 are a starting point in the design process and further refinement of the coil winding is expected as issues such as quench protection and a risk assessment of the LTS magnets relative to the MPEX design are considered in greater detail.

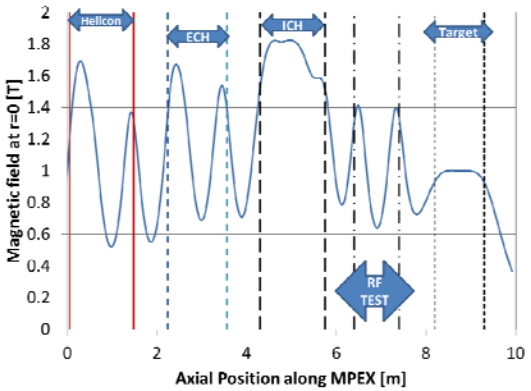

Figure 3. Axial field profile along MPEX with different regions of MPEX operation highlighted.

4. MPEX Refrigeration Considerations

For the cryogenic cooling of the MPEX superconducting magnets, separate, liquid helium condensing cryocooler systems were chosen over a closed cycle, reverse-Brayton liquid helium refrigeration system. First, given the modular nature of the MPEX assembly and potential maintenance and access required for the different supporting systems, the ability to remove each magnet system without having to disconnect transfer lines is an advantage that could also reduce the potential contamination of the closed cycle cooling system. Next, separate cryocoolers as re-condensers that operate in fairly static manner reduce the number of moving parts for the circulation pumps and valving that would be present on a liquid helium refrigeration system. This increases reliability and availability of the system. Another benefit to the cryocooler-based system is the lack of complexity that comes with a closed cycle, liquid helium refrigeration system with intricate filtering, heat exchangers, and processing of the return flow from the superconducting coils that adds additional control and monitoring and maintenance. Finally, the cost of the cryo-coolers as a whole is smaller

than a factor of two in terms of initial capital cost of a closed loop liquid helium system and by a factor of five to ten for steady state operations in terms of reduction in manpower and maintenance for the system.

Table 1. Summary of LTS coil physical and electrical coil parameters for MPEX. *L* is the coil total inductance.

Section		Warm Bore Diam. [cm]	Coil ID [cm]	Coil OD [cm]	Coil Height [cm]	L [H]	I_{op} [A]	Current Density, J_e [A/m^2]	Peak winding field [T]	Length of conductor [km]
Helicon	H1	43.2	59.3	61.8	10.2	10.7	200	4.55×10^8	3	3.8
	H2	43.2	59.3	61.8	10.2	10.7	200	4.55×10^8	3	3.8
	H3	43.2	59.3	61.3	10.2	2.6	125	3.41×10^8	2.4	1.9
	H4	43.2	59.3	61.3	15.2	5.3	125	3.41×10^8	3.3	2.9
ECH	E1	43.2	59.3	69.5	10.2	194.1	60	1.36×10^8	3	16.5
	E2	43.2	59.3	69.5	6.3	82.9	60	1.36×10^8	2.4	10.3
	E3	43.2	59.3	69.5	6.3	82.9	70	1.59×10^8	2.4	10.3
	E4	43.2	59.3	69.5	6.3	82.9	78	1.76×10^8	2.7	10.3
	E5	43.2	59.3	69.5	6.3	82.9	110	2.50×10^8	3.9	10.3
ICH	I1	43.2	59.3	61.8	63.5	13.6	83	1.80×10^8	1.9	24
	I2	43.2	59.3	61.8	69.6	13.6	87	1.73×10^8	1.9	26
	I3	43.2	59.3	61.8	10.2	10.4	120	2.73×10^8	2.4	3.8
	I4	43.2	59.3	61.8	15.4	10.4	128	2.90×10^8	2.5	3.8
RF Test Area	R1	43.2	59.3	64.4	5.1	12.9	150	3.41×10^8	3.8	3.9
	R2	43.2	59.3	64.4	5.1	12.9	150	3.41×10^8	3.8	3.9
	R3	43.2	59.3	64.4	5.1	12.9	140	3.18×10^8	3.8	3.9
	R4	43.2	59.3	64.4	5.1	12.9	140	3.18×10^8	2.8	3.9
Target	T1	115.0	131.5	134.6	40.0	178	68	1.55×10^8	1.5	85
	T2	115.0	131.5	133.4	42.0	68	68	1.55×10^8	1.0	89
	T3	115.0	131.5	134.6	42.0	191	68	1.55×10^8	1.5	89

In the analysis of heat loads for MPEX magnets during steady state operation, three different contributions were considered for the cryogenic envelope shown in figure 4. The first source was from the conduction and joule heating from current leads. From room temperature to the 40 K thermal shield, the minimum heat load for a single heat lead from McFee [24] is approximately 0.042 W/A. This would translate to first stage heat loads between 5.7 W to 16.8 W for the pairs of current leads operating over the range of currents listed in table 1. For the current lead heat leak from 40 K to 4.2 K, conduction cooled, high temperature superconducting current leads would be utilized. Given that the only heat leak would come from the conduction between 40 K and 4.2 K as long as the current was below the current lead critical current, a heat leak per pair was estimated to be 0.1 W assuming two stainless laminated YBCO coated conductors of length 15 cm, width 0.4 cm, and thickness of 0.1 mm. This is consistent with estimates that are given in other references [25-26].

The next source of heat load is from the mechanical support of the magnets that are used to support the weight of the magnets and mitigate the axial forces that the magnets experience from interaction with one another. For purposes of this first order calculation, it is assumed that the mechanical support is provided with G10, a high strength, multilayer resin impregnated laminate. With approximately 5

cm between the cryostat inner wall and the 40 K thermal shield, the heat load was estimated with the following expression

$$Q_{\sup port} = \frac{A_{g10}}{L_{g10}(5cm)} \int_{T_l=40K/4.2K}^{T_h=300K/40K} k_{g10}(T)dT \quad (1)$$

For G10, the integrated thermal conductivity $\int k_{g10}(T)dT$ is 100 W/m from 290 K to 40 K and 5.7 W/m for 40 K to 4.2 K [27]. With the length L_{g10} fixed for mechanical supports on each side of 40 K thermal shield, the area A_{g10} is estimated by the dividing the net axial force for each cryostat by the tensile strength of G10, which is 400 MPa [28]. For the axial force between 1.59 x 10^4 N and 1.63 x 10^5 N, this would translate to an effective area A_{g10} between 0.39 cm^2 and 4 cm^2. Now since the weight of the thermal shield, inner vessel, and magnet need to be supported and ranges between 150 kg and 3200 kg, the first order maximum shear stress on the G10 supports would be 120 MPa, which well below the ultimate shear strength of G10, 130 MPa [28]. For the effective area A_{g10} listed above, the heat leak would be between 8 W and 80 W for the first stage from 290 K to 40 K and 0.4 W and 4 W for the second stage. These calculations were based on a first order approximation for the axial forces and weight of the cryogenic structure and using solid 5 mm diameter G10 rods with the number of supports linearly proportional to the axial load and weight. Further refinement during the next design phase of the project is expected to determine whether this heat load can be reduced.

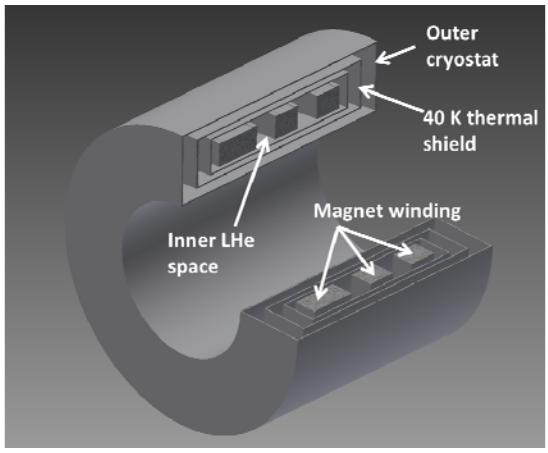

Figure 4. Cryogenic envelope for calculation of heat loads for helium recondensing-based MPEX magnets**.**

The final component of heat load is the radiation heat load between the outer cryostat and thermal shield and thermal shield to the inner LHe space where the magnets are cooled with liquid helium. Assuming an effective thermal conductivity of 37x10^{-6} W/m-K for MLI with 6 μm thick aluminium foil and 15 μm fiberglass paper spacing at 10^{-5} Torr, the radiation heat lead was calculated from the effective conduction between each surface. The nominal axial spacing between each surface was 4.6 cm and nominal radial spacing between each surface was 2.54 cm. Table 4 summarizes the individual radiation contributions to the total heat load for each cryostat as well as the current lead and mechanical support heat load. The number of cryocoolers for each cryostat was estimated assuming a Cryomech Inc. PT415 pulse tube cryocooler with a 1st stage cooling capacity of 40 W at 40 K and 1.5 W and 4.2 K [29].

Table 2. Summary of cryostats, cryo-coolers, and calculated radiation, current lead, and mechanical support heat loads for MPEX magnet system.

Cryostat	Coils		Radiation Heat Load [W]	Current Lead Heat Load [W]	Mech. Support Heat Load [W]	Total Heat Load [W]	Est. No. of Cryo-coolers	Size of LHe Reservoir
1	H1, H2, H3	*1st*	1.29	46.40	7.01	54.70	2	80 L
		2nd	0.11	0.30	0.44	0.85		
2	H4	*1st*	0.56	12.65	3.50	16.72	1	40 L
		2nd	0.04	0.10	0.22	0.36		
3	E1, E2, E3	*1st*	1.06	16.03	21.02	38.11	2	210 L
		2nd	0.10	0.30	1.34	1.74		
4	E4, E5	*1st*	0.74	24.47	12.61	37.82	1	70 L
		2nd	0.07	0.20	0.80	1.07		
5	I1, I2, I3, I4	*1st*	1.42	34.00	31.53	66.95	2	112 L
		2nd	0.14	0.40	2.00	2.54		
6	RF1, RF2	*1st*	0.54	25.31	7.01	32.86	1	33 L
		2nd	0.04	0.20	0.44	0.68		
7	RF3, RF4	*1st*	0.54	23.62	7.01	31.17	1	33 L
		2nd	0.04	0.20	0.44	0.68		
8	T1, T2, T3	*1st*	5.32	14.34	40.00	59.7	3	500 L
		2nd	0.61	0.30	2.85	3.76		

One heat source that is not mentioned in this discussion but should be considered is the ac loss generated by each coil during ramp to operating current. Using the expression for AC loss given by Wilson [18] of

$$\frac{P}{V_{hys}}\left[\frac{W}{m^3}\right] = \frac{dB}{dt}\, j_c \frac{2d_f}{3\pi} \qquad (2)$$

where dB/dt is the ramp rate of the field in the coil winding, J_c is the current density of the superconductor, and d_f is the effective diameter of the superconductor, the ac loss was calculated for the volume of each coil winding and is shown for each coil in figure 7. A ramp rate of 0.01 A/s was assumed along with J_c of 2.61×10^{-9} A/m^2 and d_f of 70 μm [19]. When the number of filaments (54) and the amount of conductor for each coil is taken into account, the ac loss contribution to the LHe bath is between 0.04 W and 0.75 W. While this range is fairly manageable for pulse tube cryo-cooler arrangement, additional modelling is needed to make sure that the temperature rise within the coil structure does not result in coil quench.

While the pulse tube cryo-cooler refrigeration makes the most sense from an operations standpoint, the cool-down of the MPEX magnets during initial operation and after each long-term outage require the usage of liquid helium and possibly liquid nitrogen depending on the circumstances. Based on the thermal mass of each system, which consists of the 40 K thermal shield, the magnet, magnet supports, and the liquid helium storage, Table 3 provides the amount of liquid helium required with and without

the liquid nitrogen precooling. This shows the decided advantage with liquid nitrogen precooling. It should be noted that the amount of liquid helium and nitrogen was found by an energy balance between the enthalpy in the cold mass and the heat of vaporization for the liquid helium (20 kJ/kg) and liquid nitrogen (199.3 kJ/kg). The usage of the sensible heat of the cryogen as it warms from the saturation temperature to its surroundings will likely reduce the amount of liquid helium consumed. However given that the utilization of this sensible heat is dependent on geometry and flow rate, additional calculations will be done to determine reduction in liquid helium. Given that the majority of this liquid helium is tied to the target coil, a possible cost reduction could be found by installing a small scale refrigeration system that is separate for the target to handle the cooling of the target coils if multiple outages are planned for maintenance or configuration changes.

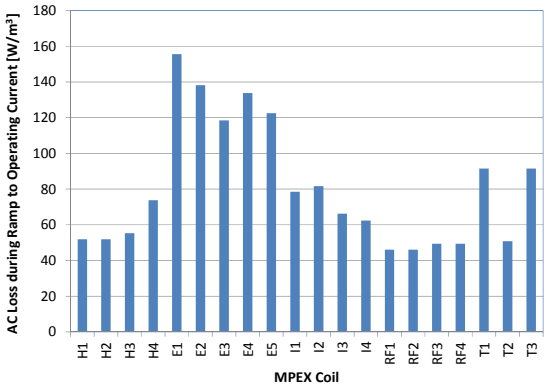

Figure 6. Estimate ac loss for each MPEX coil during ramp up to operating current.

Table 3. Summary of LHe required to bring MPEX magnets down to operating temperatures of 4.2 K with and without liquid nitrogen precooling

Cryostat	Coils	Cooldown with LN2 Precooling		Cooldown with LHE only	Estimated Cold Mass [kg]
		LN2	LHe		
1	H1, H2, H3	150 L	650 L	14750 L	423
2	H4	100 L	200 L	4970 L	157
3	E1, E2, E3	350 L	1300 L	34220 L	636
4	E4, E5	160 L	680 L	15560 L	376
5	I1, I2, I3, I4	175 L	775 L	17060 L	1860
6	RF1, RF2	100 L	375 L	9030 L	300
7	RF3, RF4	100 L	375 L	9030 L	300
8	T1, T2, T3	2050 L	8500 L	202700 L	3641

5. Conclusions and Future Design Work

A conceptual design for superconducting magnets and their supporting cryogenic system has been carried out for a MPEX steady state, linear plasma generator for fusion material characterization. This design was based on the usage of LTS magnets (NbTi) with a modular, recondensing liquid helium cryocooler-based refrigeration and is part of a larger design effort to determine the capital and operational costs for MPEX. Other elements of the MPEX design effort include the RF technology implementation from proto-MPEX, where the RF technology has been demonstrated or is under development [6-7], optimization of vacuum components, and the mechanical support structure.

Within the superconducting magnet and cryogenic system design, further refinements are on-going. While it is expected that the quench protection for the magnets should be passive, the inductance of the large target coils remain a concern. This issue will be investigated through discussions with national laboratories and industrial companies with magnet winding experience of coils of similar geometry. With respect to the superconducting materials, our initial assessment of the current status of other superconductors like MgB_2 and YBCO-based coated conductors was based on a survey of the literature over the past five years. Like the quench protection issue, discussions with national laboratories and industrial magnet and superconducting manufacturers are planned to determine the projected progress in piece length, supply, and cost that may benefit magnet construction in the next two to five years. Finally, given the tight supply of commercially available liquid helium, the consumption of liquid helium to cool the MPEX magnets remains a concern. The cost benefit analysis for cryogenic support of MPEX will be reviewed to determine whether this advantage for a closed-cycle, reverse Brayton cycle liquid helium system outweighs its drawbacks when compared to the modular, recondensing liquid helium cryocooler-based refrigeration system.

Acknowledgments

This manuscript has been authored by UT-Battelle, LLC under Contract No. DE-AC05-00OR22725 with the U.S. Department of Energy. Notice: This manuscript has been authored by UT-Battelle, LLC, under Contract No. DE-AC0500OR22725 with the U.S. Department of Energy. The United States Government retains and the publisher, by accepting the article for publication, acknowledges that the United States Government retains a non-exclusive, paid-up, irrevocable, world-wide license to publish or reproduce the published form of this manuscript, or allow others to do so, for the United States Government purposes

References

[1] Pitts R A, et al., 2011 *J. Nucl. Mater*. **415** S957
[2] Rieth M, EFDA Technical Meeting on DEMO (Garching, Germany September 29-30, 2009)
[3] Rieth M, et al., 2013 *J. Nucl. Mater.* **417** 463
[4] Behrisch R, et al., 2003 *J. Nucl. Mater*. **313-316** 388
[5] Roth J, et al., 2009 *J. Nucl. Mater*. **390-391** 1
[6] Rapp J, et al., 2013 *Fusion Sci. Technol.* **64** 237
[7] Rapp J, et al., 2015 The Material Plasma Exposure eXperiment MPEX: pre-design, development and testing of source concept *2015 IEEE 26th Symposium on Fusion Engineering*, submitted for publication.
[8] Carter M D, et al., 2002 *Phys. Plasmas* **9** 5097
[9] Mori Y, et al., 2004 *Plasma Sources Sci. Technol*. **13** 424
[10] Hooke W M, et al., 1965 *Phys. Fluids* **8** 1146
[11] Roberts D R and Hershkowitz H, 1992 *Phys. Fluids B* **4** 1475
[12] Golovato S N, et al., 1988 *Phys. Fluids* **31** 3744
[13] Golovato S N, et al., 1985 *Phys. Fluids* **28** 734
[14] Bering E A, et al., 2010 *Phys. Plasmas* **17** 043509
[15] Young E A, et al., 2015 *IEEE Trans. Appl. Supercond.* **25** 4600105
[16] Mine S, et al., 2015 *IEEE Trans. Appl. Supercond.* **25** 4600604
[17] Hahn S, et al., 2015 *IEEE Trans. Appl. Supercond.* **25** 4600405
[18] Wang X, et al., 2015 *IEEE Trans. Appl. Supercond.* **25** 4601904
[19] Oxford Instruments, Inc. http://www.oxford-instruments.com/products/superconducting-magnets-and-wire/superconducting-wire/nb-ti-copper-matrix-monolith
[20] Flex PDE, PDE Solutions Inc., http://www.pdesolutions.com/psi.html
[21] Bottura L, 2000 *IEEE Trans. Appl. Supercond.* **10** 1054
[22] Wilson M N, 1983 *Superconducting Magnets* New York, Clarendon Press
[23] Grover F W, 1962 *Inductance Calculations* New York, Dover Publications

[24] McFee, R, 1959 *Rev. Sci. Instrum.* **30** 98
[25] Iwasa Y, 2009 *Case Studies in Superconducting Magnets: Design and Operational Issues* New York, Springer-Velag
[26] Tsurudome T, et al., 2013 *IEEE Trans. Appl. Supercond.* **23** 6450060
[27] Child G, Erics L J, and Powell R L, 1973 *NBS Monograph* **131**
[28] Ekin, J W, 2006 *Experimental Techniques for Low-Temperature Measurements* New York, Oxford University Press
[29] Cryomech Inc, Syracuse, NY 13211. http://www.cryomech.com/capacitycurve/PT415_cc.pdf